

Electron Transfer Catalysis in the Activation of C–H Bonds by Iridium Complexes

Pietro Diversi,^{*,†} Stefania Iacononi,[†] Giovanni Ingrosso,[†] Franco Laschi,[‡]
Antonio Lucherini,[†] Calogero Pinzino,[§] Gloria Uccello-Barretta,^{||} and
Piero Zanello[‡]

Dipartimento di Chimica e Chimica Industriale, Università di Pisa, Via Risorgimento 35, 56126 Pisa, Italy, Dipartimento di Chimica, Università di Siena, Pian dei Mantellini 44, 53100 Siena, Italy, Istituto di Chimica Quantistica ed Energetica Molecolare del CNR, Via Risorgimento 35, 56126 Pisa, Italy, and Centro del CNR per lo Studio delle Macromolecole Stereoordinate ed Otticamente Attive, Via Risorgimento 35, 56126 Pisa, Italy

Received January 26, 1995[®]

Iridium(III) dimethyl complexes, $\text{Cp}^*\text{Ir}(\text{PR}_3)_2\text{Me}_2$ ($\text{Cp}^* = \eta^5\text{-C}_5\text{Me}_5$; $\text{R} = \text{Ph}$ (**1a**), Me (**1b**), react slowly (**1a**), or not at all (**1b**), with C–H bonds of aromatic hydrocarbons under severe conditions (110 °C, 2 weeks) to give methane and the new methyl aryl derivatives $\text{Cp}^*\text{Ir}(\text{PPh}_3)(\text{Me})(\text{Ar})$ ($\text{Ar} = \text{C}_6\text{H}_5$, $\text{C}_6\text{H}_4\text{Me}$, $\text{C}_6\text{H}_4\text{CF}_3$, $\text{C}_6\text{H}_3\text{Me}_2$). With benzene and trifluorotoluene, the diaryl complexes $\text{Cp}^*\text{Ir}(\text{PPh}_3)_2\text{Ar}_2$ are also formed. In contrast, the reaction of both **1a** and **1b** with arenes, in the presence of catalytic amounts of an oxidant ($\text{Cp}_2\text{Fe}^+\text{PF}_6^-$, AgBF_4 , or $\text{Ph}_3\text{C}^+\text{BF}_4^-$), proceeds rapidly at room temperature: the corresponding methyl aryl derivatives $\text{Cp}^*\text{Ir}(\text{PR}_3)(\text{Me})(\text{Ar})$ ($\text{R} = \text{Ph}$; $\text{Ar} = \text{C}_6\text{H}_5$, C_6D_5 , $\text{C}_6\text{H}_4\text{Me}$, $\text{C}_6\text{H}_4\text{CF}_3$, $\text{C}_6\text{H}_3\text{Me}_2$. $\text{R} = \text{Me}$; $\text{Ar} = \text{C}_6\text{H}_5$, C_6D_5 , $\text{C}_6\text{H}_4\text{Cl}$, $\text{C}_6\text{H}_4\text{Br}$, $\text{C}_6\text{H}_4\text{F}$, $\text{C}_6\text{H}_4\text{CF}_3$, $\text{C}_6\text{H}_4\text{NO}_2$, $\text{C}_6\text{H}_4\text{Me}$, $\text{C}_6\text{H}_3\text{Me}_2$) are produced. In the reaction with benzene- d_6 , a mixture of CH_4 and CH_3D is obtained. When substituted arenes are used, only the meta and para C–H bonds react. In the case of **1a**, the methyl aryl derivative is in equilibrium with the orthometalated compound $\text{Cp}^*\text{Ir}(\text{C}_6\text{H}_4\text{PPh}_2)(\text{Me})$ (**12**), which is the primary reaction product. Evidence is provided for a facile one-electron oxidation of **1a** and **1b**. The electrochemical oxidation of **1a**, **1b**, and related iridium(III) dialkyls in CH_2Cl_2 involves a 1-electron process, yielding the corresponding iridium(IV) paramagnetic cations, as shown by coupled electrochemical–ESR studies. AgBF_4 oxidation of **1a** and **1b** in CH_2Cl_2 gives instead radical species, which have been shown by ESR spectroscopy to have the “tucked-in” structure $\text{Ir}(\eta^5\text{-C}_5\text{Me}_4\text{CH}_2)$. Such species are proved to be involved as intermediates in the above arene C–H activation reactions.

Introduction

The role of odd-electron species in transition-metal organometallic chemistry has only been fully recognized recently despite the pioneering studies by Kochi.¹ Odd-electron complexes may have reactivity patterns, which are forbidden for species obeying the 16/18-electron rule but which proceed easily through radical (mainly 17- and 19-electron) intermediates.^{1d,f,g} Taking advantage of these ideas, it has been shown that many reactions, such as ligand substitution,² CO insertion,³ and isomerizations of complexes,⁴ which occur slowly for 18-electron closed-shell species, may be dramatically accelerated in the presence of electron transfer reagents, which can give rise to 17- and 19-electron intermediates.

In the course of our investigations on the cyclometalation reactions of half-sandwich iridium(III) dialkyl derivatives,^{5a,b} we have found that the methyl complexes $\text{Cp}^*\text{Ir}(\text{PR}_3)_2\text{Me}_2$ ($\text{R} = \text{Ph}$ (**1a**), Me (**1b**)), which are able to activate C–H bonds of arenes only under rather drastic conditions or not at all, become strongly reactive in the presence of catalytic amounts of one-electron oxidants.^{5c} These C–H activation reactions have features which make them analogous to the “ σ -bond metathesis”⁶ of M–R bonds and hydrocarbon C–H

[†] Università di Pisa.

^{||} Università di Siena.

[§] Istituto di Chimica Quantistica ed Energetica Molecolare del CNR.

^{||} Centro del CNR per lo Studio delle Macromolecole Stereoordinate ed Otticamente Attive.

[®] Abstract published in *Advance ACS Abstracts*, May 15, 1995.

(1) (a) Kochi, J. K. *Organometallic Mechanism and Catalysis*; Academic Press: New York, 1978. (b) Chanon, M.; Tobe, M. L. *Angew. Chem., Int. Ed. Engl.* **1982**, *21*, 1. (c) Astruc, D. *Angew. Chem., Int. Ed. Engl.* **1988**, *27*, 643. (d) Astruc, D. *Chem. Rev.* **1988**, *88*, 1189. (e) Tyler, D. R. *Prog. Inorg. Chem.* **1988**, *36*, 125. (f) Tyler, D. R. *Acc. Chem. Res.* **1991**, *24*, 325. (g) Astruc, D. *Acc. Chem. Res.* **1991**, *24*, 36.

(2) Kochi, J. K. *J. Organomet. Chem.* **1986**, *300*, 139.

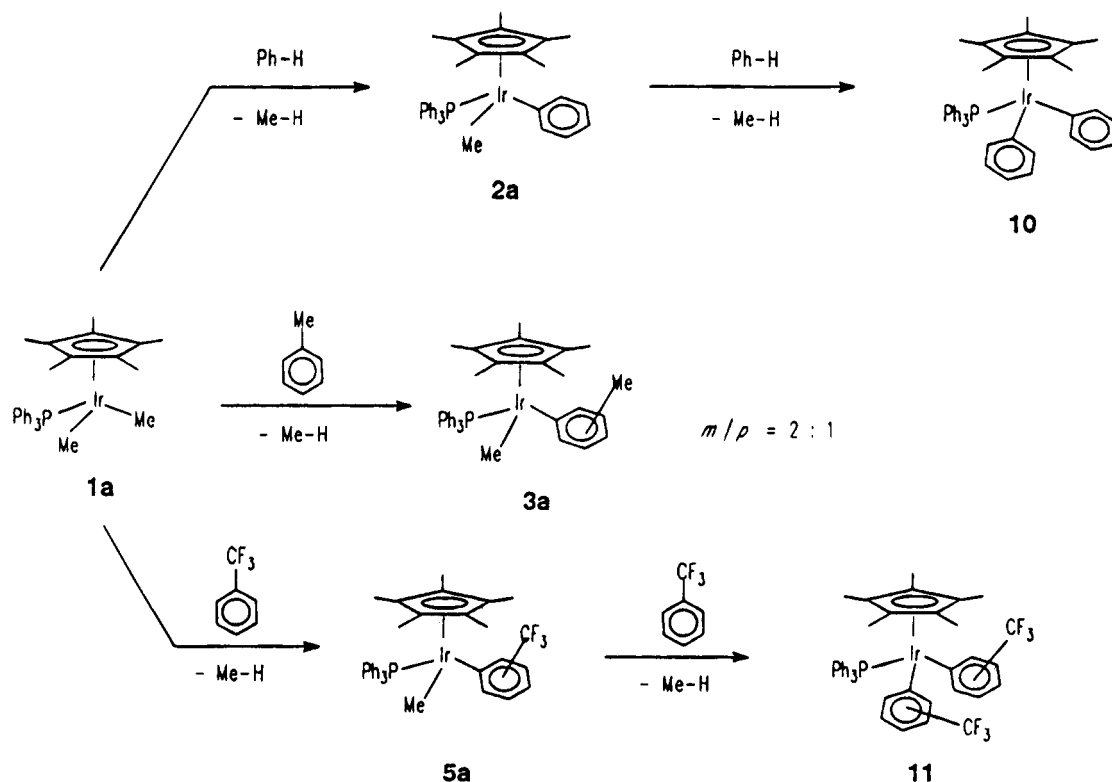
(3) (a) Magnuson, R. H.; Meirowitz, R.; Zulu, S.; Giering, P. *J. Am. Chem. Soc.* **1982**, *104*, 5790. (b) Magnuson, R. H.; Meirowitz, R.; Zulu, S. J.; Giering, W. P. *Organometallics* **1983**, *2*, 460. (c) Therien, M. J.; Troglor, W. C. *J. Am. Chem. Soc.* **1987**, *109*, 5127. (d) Prock, A.; Giering, W. P.; Greene, J. E.; Meirowitz, R. E.; Hofmann, S. L.; Woska, D. C.; Wilson, M.; Chang, R.; Chen, J.; Magnuson, R. H.; Eriks, K. *Organometallics* **1991**, *10*, 3479.

(4) (a) Bond, A. M.; Colton, R.; Mann, T. F. *Organometallics* **1988**, *7*, 749. (b) Bond, A. M.; Colton, R.; Feldberg, S. W.; Mahon, P. J.; Whyte, T. *Organometallics* **1991**, *10*, 3320.

(5) (a) Andreucci, L.; Diversi, P.; Ingrosso, G.; Lucherini, A.; Marchetti, F.; Adovasio, V.; Nardelli, M. *J. Chem. Soc., Dalton Trans.* **1986**, 803. (b) Diversi, P. *Abstracts of the Italian-Portuguese-Spanish Meeting in Inorganic Chemistry*, Gandia (Valencia), Spain, June 25–29, 1990; p 60. (c) Diversi, P.; Iacononi, S.; Ingrosso, G.; Laschi, F.; Lucherini, A.; Zanello, P. *J. Chem. Soc., Dalton Trans.* **1993**, 351.

(6) (a) Watson, P. L.; Parshall, G. W. *Acc. Chem. Res.* **1985**, *18*, 51. (b) Fendrick, C. M.; Marks, T. J. *J. Am. Chem. Soc.* **1986**, *108*, 425. (c) Thompson, M. E.; Baxter, S. E.; Ray Bulls, A.; Burger, B. J.; Nolan, M. C.; Santarsiero, B. D.; Schaefer, W. P.; Bercaw, J. E. *J. Am. Chem. Soc.* **1987**, *109*, 203. (d) Rothwell, I. P. In *Activation and Functionalization of Alkanes*; Hill, C. L., Ed.; Wiley: New York, 1989; p 151.

Scheme 1



bonds (eq 1). This reaction has been more commonly



observed for early transition or f-block⁶ and also for a few late⁷ transition metals under conditions of thermal activation.

Since the oxidation behavior of **1a** and **1b** is peculiar if compared with that of other one-electron oxidative cleavages of metal-carbon bonds reported in the literature for late d-block metals, e.g., organoruthenium,⁸ organocobalt,⁹ organorhodium,^{9c,10} organopalladium,¹¹ and organoplatinum¹² complexes, we decided to study more thoroughly the chemical and electrochemical oxidation of **1a** and **1b** both in the presence and in absence of arenes. The results of this study compared with the data of the thermolysis of **1a** and **1b** in arenes are reported in this paper.¹³

Results and Discussion

Thermolysis of 1a and 1b. The reactivity of **1a** and **1b** toward arenes has been studied under conditions of

(7) (a) Gomez, M.; Yarrow, P. I.; Robinson, D. J.; Maitlis, P. M. *J. Organomet. Chem.* **1985**, 279, 115. (b) Lehmkuhl, H.; Bellenbaum, M.; Grundke, J.; Mauermann, H.; Krüger, C. *Chem. Ber.* **1988**, 121, 1719. (c) Lehmkuhl, H.; Schwickardi, R.; Mehler, G.; Krüger, C.; Goddard, R. Z. *Anorg. Allg. Chem.* **1991**, 606, 141.

(8) Aase, T.; Tilset, M.; Parker, V. D. *J. Am. Chem. Soc.* **1990**, 112, 4974.

(9) (a) Witman, M. W.; Weber, J. H. *Inorg. Chim. Acta* **1977**, 23, 263. (b) Tambllyn, W. H.; Klingler, R. J.; Hwang, W. S.; Kochi, J. K. *J. Am. Chem. Soc.* **1981**, 103, 3161. (c) Åkermarck, B.; Almemark, M.; Jutand, A. *Acta Chem. Scand.* **1982**, B36, 451. (d) Vol'pin, M. E.; Levitin, I. Ya.; Sigau, A. L.; Nikitaev, A. T. *J. Organomet. Chem.* **1985**, 279, 263. (e) Fukuzumi, S.; Ishikawa, K.; Tanaka, T. *J. Chem. Soc., Dalton Trans.* **1985**, 899.

(10) Pedersen, A.; Tilset, M. *Organometallics* **1993**, 12, 56.

(11) Seligson, A. L.; Troglor, W. C. *J. Am. Chem. Soc.* **1992**, 114, 7085.

(12) Chen, J. Y.; Kochi, J. K. *J. Am. Chem. Soc.* **1977**, 99, 1450.

(13) (a) When this paper was at the point of being submitted for publication, a study of the oxidation chemistry of $\text{Cp}^*\text{Ir}(\text{PPh}_3)_2\text{Me}_2$ (**1a**) in acetonitrile was reported.^{13b} Owing to the coordination ability of acetonitrile, the reactivity is quite different from that described here.

(b) Pedersen, A.; Tilset, M. *Organometallics* **1994**, 13, 4887.

(14) Tolman, C. A. *Chem. Rev.* **1977**, 77, 313.

thermal activation. While **1b** is stable for months toward aliphatic and aromatic hydrocarbons at temperatures up to 140 °C (above this temperature decomposition starts to be significant), **1a** reacts slowly with arenes at temperatures higher than 70 °C; the thermolysis has been typically studied at 110 °C, this temperature providing a convenient reaction rate without appreciable decomposition (Scheme 1). Reaction with benzene gives methane and the methyl phenyl complex **2a**, which reacts further with benzene to give methane and the diphenyl derivative **10**.

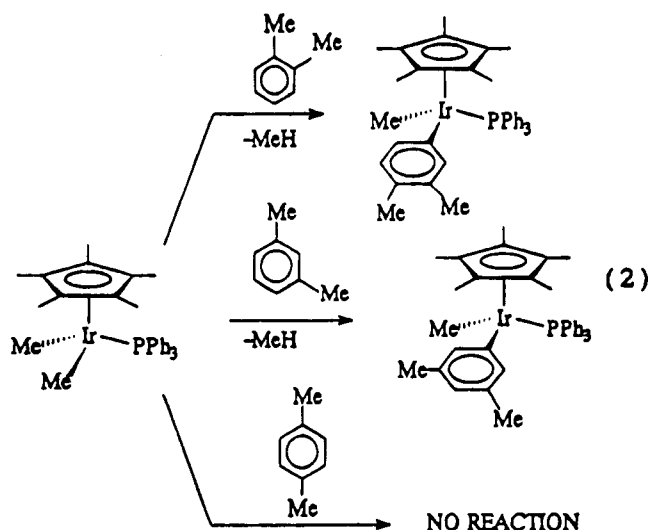
The reaction with benzene-*d*₆ is conveniently followed by ¹H NMR spectroscopy, and it is well described by a pseudo-first-order kinetic law for over 4 half-lives ($k = 2.55 \times 10^{-2} \text{ h}^{-1}$, $t_{1/2} = 27.2 \text{ h}$, $110 \pm 0.5 \text{ °C}$), **1a** being completely converted after 2 weeks. Since only MeD is formed and no intramolecular activation product has been detected, we suggest the hypothesis of a reaction intermediate deriving from the temporary loss of triphenylphosphine. This is consistent also with the complete inhibition of the reaction by an excess of free phosphine ($\text{PPh}_3/\text{1a} = 4$) and with the thermal stability of **1b**, which is presumably only slightly dissociated in solution because of the smaller cone angle of trimethylphosphine with respect to the bulky triphenylphosphine.¹⁴ Analogously Maitlis et al.^{7a} have proposed that, in reactions of arene thermal activation by the related complex $\text{Cp}^*\text{Ir}(\text{DMSO})\text{Me}_2$ (DMSO = dimethyl sulfide), the loss of the DMSO ligand is a prerequisite for the oxidative addition of the arene C-H bond.

1a is able to activate other arenes (Scheme 1). The reaction of toluene is slightly slower than that of benzene ($k = 2.32 \times 10^{-2} \text{ h}^{-1}$, first-order rate law, $t_{1/2} = 29.9 \text{ h}$, in the case of toluene-*d*₈, by ¹H NMR spectroscopy), and the reaction product is a mixture of the *m*- and *p*-tolyl derivatives **3a** in a 2/1 ratio. The two isomers were identified by analysis of the ¹H NMR spectra of the reaction mixtures and by comparison with

the spectra of authentic samples prepared by stepwise alkylation of the dichloro complex $\text{Cp}^*\text{Ir}(\text{PPh}_3)\text{Cl}_2$. There is no evidence for the activation of the *ortho*, and benzyl C-H bonds, as well as for the formation of a diaryl complex.

Trifluorotoluene behaves like benzene since the methyl trifluorotolyl derivatives *m*- and *p*-**5a** (3/2 mixture) initially formed react further with the arene to be converted into the diaryl isomers **11** (95%, after 2 weeks at 110 °C). The regiochemistry of both reaction steps seems to be regulated by steric effects, only the *meta* and *para* C-H bonds being activated. The three major diaryl isomers **11** (four isomers have been actually detected, one of these being present in very low amounts) have not been isolated, and the mixture has been analyzed by ^1H NMR two-dimensional exchange (NOE-SY) spectroscopy, in benzene- d_6 solution at 25 °C. As shown in Table 1, the Cp^* protons gave distinct resonances for the three isomers at 1.19, 1.16, and 1.13 ppm; each of them gives rise to intramolecular interligand NOEs on the aromatic protons of the trifluorotolyl groups, thus allowing us to perform a complete structural assignment. The Cp^* protons at δ 1.19 gave NOEs only on the singlet at δ 7.95 and on the doublet at δ 7.42 and hence were attributed to the isomer containing two *m*-trifluorotolyl groups (**m,m'**-**11**). The Cp^* protons at δ 1.13, which gave NOEs only on the doublet at δ 7.01, were assigned to the isomer containing two *para*-substituted aromatic groups (**p,p'**-**11**). Finally, the Cp^* methyls at δ 1.16 originated the most complex NOE pattern: at δ 7.96 (singlet), 7.02 (doublet), and 7.41 (doublet); the signals at δ 7.02 and 7.41 showed *J*-coupling with the triplet at δ 6.60 and with the doublet at δ 7.05, respectively, thus indicating that this isomer contains one *m*- and one *p*-trifluorotolyl group (**m,p'**-**11**).

1a was also reacted with xylenes, giving selectively and almost quantitatively the methyl aryl derivative **m,m**-**4a** in the case of *m*-xylene and the **m,p**-**4a** isomer from *o*-xylene (*p*-xylene does not react at all) (eq 2).



These results clearly show the importance of steric factors on the course of the reaction and in particular the inertia of the C-H bonds *ortho* to the substituents.

Oxidatively Promoted Arene C-H Activation by **1a and **1b**.** Treatment of **1a** with benzene in the presence of small amount. (10–15%) of $\text{Cp}_2\text{Fe}^+\text{PF}_6^-$ produces, after an induction period of a few seconds, a

rapid evolution of gas and a transient red-violet color at the solid-oxidant surface. Monitoring the reaction by ^1H NMR, we have observed the formation of ferrocene and CH_4 together with a new organometallic compound, which has been identified as the orthometal-

lated complex $\text{Cp}^*\text{Ir}(\text{C}_6\text{H}_4\text{PPh}_2)\text{Me}$ (**12**) (92% after 2 h) (Scheme 2). In fact the aromatic region of the ^1H NMR spectrum shows the typical pattern of the orthometalated triphenylphosphine, and the high-field resonance in the ^{31}P NMR spectrum ($\delta = -57.50$ in benzene- d_6) is consistent¹⁵ with the presence of a phosphorus atom in a four-membered ring (Table 1). Compound **12**, which is stable for months in benzene at 110 °C, when left in the presence of the oxidant, adds benzene, thus restoring the monohapto phosphine ligand and giving $\text{Cp}^*\text{Ir}(\text{PPh}_3)(\text{Me})(\text{Ph})$ (**2a**), which has been characterized by comparison with an authentic sample prepared by sequential alkylation of $\text{Cp}^*\text{Ir}(\text{PPh}_3)\text{Cl}_2$ first with MeMgI and then with PhMgBr . By monitoring the reaction with ^1H NMR, one finds that a maximum of 85% conversion of **12** in **2a** is reached after 16 h. The same product ratio (**2a**/**12** = 85/15) has been obtained by reaction of pure **2a** or **12** in benzene- d_6 in the presence of the oxidant. If the concentrations of **2a** and **12** are expressed as molar fractions, then $K_{\text{eq}} = \chi_{12}\chi_{\text{C}_6\text{H}_6}/\chi_{2a} = 0.18$ (molar $K_{\text{eq}} = 2.0$ M) and $\Delta G^\circ = 1.01$ kcal/mol (as a term of comparison, see the data by Jones and Feher for the reaction $\text{Cp}^*\text{Rh}(\text{PMe}_2\text{CH}_2\text{Ph})(\text{Ph})\text{H} \rightleftharpoons \text{Cp}^*\text{Rh}$ -

$(\text{C}_6\text{H}_4\text{CH}_2\text{PMe}_2)\text{H} + \text{PhH}$, in which a relatively more stable five-membered ring is involved: $K_{\text{eq}} = 36.7$, $\Delta G^\circ = -2.32$ kcal/mol).¹⁶ This shows that the intermolecular reaction product **2a** is thermodynamically favored and that the intramolecular C-H activation product **12** is only kinetically preferred.

Pure **12** can be conveniently prepared and isolated by reaction of **1a** in dichloromethane in the presence of the ferrocenium cation: only the intramolecular activation product **12** is obtained, and no reaction with the solvent takes place.

The amount of $\text{Cp}_2\text{Fe}^+\text{PF}_6^-$ necessary to catalyze the reaction is only a fraction of the quantity employed, corresponding to 4–6% of the moles of **1a**, as evaluated by ^1H NMR on the basis of the ferrocene which is formed. A saturated benzene solution of the poorly soluble ferrocenium salt catalyzes the cyclometalation of **1** to **12** (although *ca.* 10^2 times less rapidly than in the presence of solid oxidant) but is not able to induce further reaction of **12** with benzene. In the presence of the ferrocenium salt, **1a** reacts also with several other arenes (toluene, xylenes, trifluorotoluene) to give the corresponding methyl aryl derivative *via* the formation of the intramolecular activation product **12**. The presence of the substituent on the ring introduces a complication due to the isomerism. The products have been identified by analysis of the $^1\text{H}\{^1\text{H}\}$ NOE difference or 2D NOESY spectra (benzene- d_6 , 25 °C), as previously described in detail for isomers **11**. The NMR spectral data are reported in Table 1. Part of the structural assignments were made by comparison with authentic samples prepared by a different route (see Experimental

(15) Garrou, P. E. *Chem. Rev.* **1981**, *81*, 229.

(16) (a) Jones, W. D.; Feher, F. J. *J. Am. Chem. Soc.* **1984**, *106*, 1650. (b) Jones, W. D.; Feher, F. J. *J. Am. Chem. Soc.* **1985**, *107*, 620. (c) Jones, W. D. In *Activation and Functionalization of Alkanes*; Hill, C. L., Ed.; Wiley: New York, 1989; p 111.

Table 1. NMR Spectral Data^a

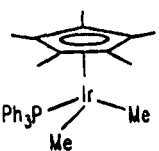
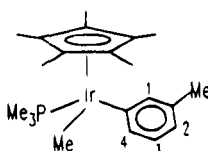
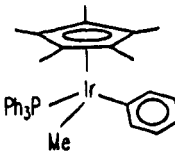
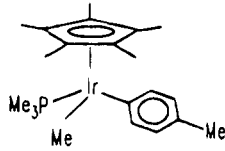
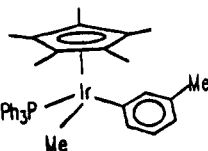
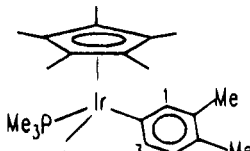
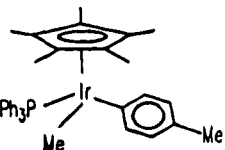
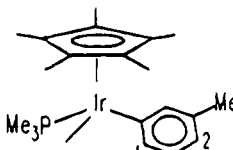
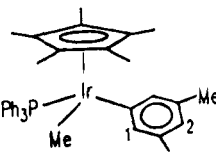
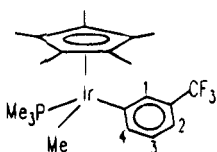
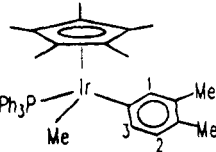
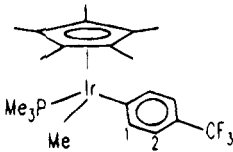
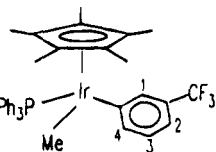
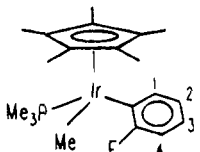
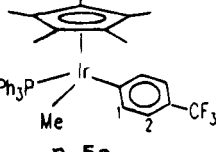
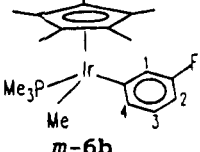
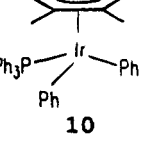
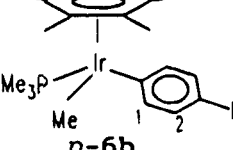
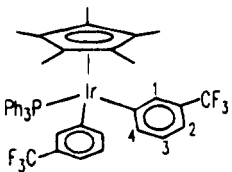
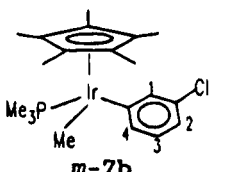
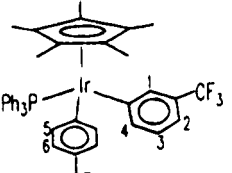
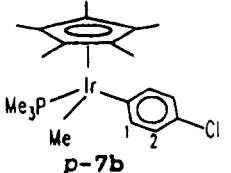
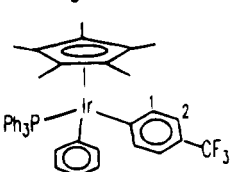
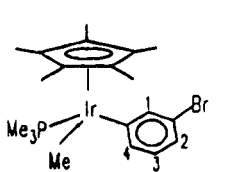
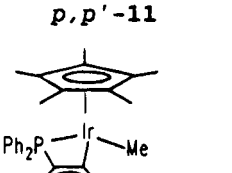
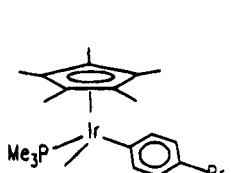
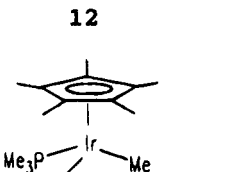
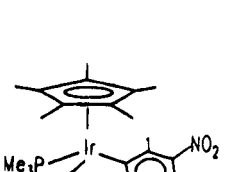
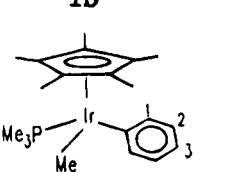
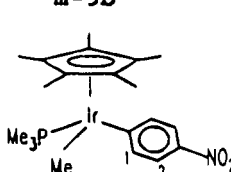
	¹ H	³¹ P		¹ H	³¹ P
 1a	0.64 [d, 6 H, <i>J</i> (PH) 5.0, Ir-Me] 1.40 [d, 15 H, <i>J</i> (PH) 1.9, C ₅ Me ₅] 6.95–7.15 (m, 9 H, PPh ₃) 7.44–7.56 (m, 6 H, PPh ₃)	10.77	 m-3b	0.64 [d, 3 H, <i>J</i> (PH) 6.7, Ir-Me] 0.99 [d, 9 H, <i>J</i> (PH) 9.8, PMe ₃] 1.52 [d, 15 H, <i>J</i> (PH) 1.8, C ₅ Me ₅] 2.36 (s, 3 H, Me) 7.4–7.85 (m, 4 H, H ₁ + H ₂ + H ₃ + H ₄)	
 2a	0.86 [d, 3 H, <i>J</i> (PH) 6.0, Ir-Me] 1.34 [d, 15 H, <i>J</i> (PH) 1.8, C ₅ Me ₅] 6.8–7.5 (m, 20 H, PPh ₃ + Ph)	10.72	 p-3b	0.62 [d, 3 H, <i>J</i> (PH) 6.7, Ir-Me] 0.99 [d, 9 H, <i>J</i> (PH) 9.7, PMe ₃] 1.52 [d, 15 H, <i>J</i> (PH) 1.8, C ₅ Me ₅] 2.33 (s, 3 H, Me) 7.01 [d, <i>J</i> (HH) 7.7, H ₂] 7.38 [d, 2 H, <i>J</i> (PH) 7.9, H ₁]	
 m-3a	0.89 [d, 3 H, <i>J</i> (PH) 6.0, Ir-Me] 1.36 [d, 15 H, <i>J</i> (PH) 1.8, C ₅ Me ₅] 2.17 (s, 3 H, Me) 6.8–7.35 (m, 19 H, Ph)	10.89	 m, p-4b	0.66 [d, 3 H, <i>J</i> (PH) 6.6, Ir-Me] 1.01 [d, 9 H, <i>J</i> (PH) 9.6, PMe ₃] 1.54 [d, 15 H, <i>J</i> (PH) 1.8, C ₅ Me ₅] 2.24 (s, 3 H, Me) 2.29 (s, 3 H, Me) 6.97 [d, 1 H, <i>J</i> (HH) 7.5, H ₂] 7.01 [d, <i>J</i> (HH) 7.7, H ₃] 7.23 (s, 1 H, H ₁)	-38.07
 p-3a	0.89 [d, 3 H, <i>J</i> (PH) 6.0, Ir-Me] 1.36 [d, 15 H, <i>J</i> (PH) 1.8] 2.25 (s, 3 H, Me) 6.8–7.35 (m, 19 H, Ph)	10.67	 m, m-4b	0.66 [d, 3 H, <i>J</i> (PH) 6.6, Ir-Me] 1.01 [d, 9 H, <i>J</i> (PH) 9.7, PMe ₃] 1.54 [d, 15 H, <i>J</i> (PH) 1.8, C ₅ Me ₅] 2.36 (s, 6 H, Me) 6.73 (s, 2 H, H ₁) 7.16 (s, 1 H, H ₂)	
 m, m-4a	0.88 [d, 3 H, <i>J</i> (PH) 5.9, Ir-Me] 1.38 [d, 15 H, <i>J</i> (PH) 1.7, 15 H] 2.19 (s, 6 H, Me) 6.64 (s, 1 H, H ₂) 6.92 (s, 2 H, H ₁) 6.95–7.10 (m, 15 H, PPh ₃)		 m-5b	0.52 [d, 3 H, <i>J</i> (PH) 6.8, Ir-Me] 0.88 [d, 9 H, <i>J</i> (PH) 9.7, PMe ₃] 1.41 [d, 15 H, <i>J</i> (PH) 1.8, C ₅ Me ₅] 6.97 [t, 1 H, <i>J</i> (HH) 7.8, H ₃] 7.31 [d, 1 H, <i>J</i> (HH) 7.8, H ₂] 7.52 [d, 1 H, <i>J</i> (HH) 8.0, H ₄] 7.84 (s, 1 H, H ₃)	-38.36
 m, p-4a	0.89 [d, 3 H, <i>J</i> (PH) 6.0, Ir-Me] 1.37 [d, 15 H, <i>J</i> (PH) 1.8, C ₅ Me ₅] 2.08 (s, 3 H, Me) 2.19 (s, 3 H, Me) 6.87 [d, 1 H, <i>J</i> (HH) 8.1, H ₂] 7.02 (s, 1 H, H ₁) 7.14 [d, 1 H, <i>J</i> (HH) 7.9, H ₃] 6.95–7.10 (m, 15 H, PPh ₃)	10.77	 p-5b	0.50 [d, 3 H, <i>J</i> (PH) 7.1, Ir-Me] 0.86 [d, 9 H, <i>J</i> (PH) 9.5, PMe ₃] 1.40 [d, 15 H, <i>J</i> (PH) 1.8, C ₅ Me ₅] 7.32 [d, 2 H, <i>J</i> (HH) 8.2, H ₂] 7.43 [d, 2 H, <i>J</i> (HH) 8.2, H ₁]	-38.48
 m-5a	0.78 [d, 3 H, <i>J</i> (PH) 5.9, Ir-Me] 1.27 [d, 15 H, <i>J</i> (PH) 1.8, C ₅ Me ₅] 6.86 [t, 1 H, <i>J</i> (HH) 7.8, H ₃] 7.30 [d, 1 H, <i>J</i> (HH) 7.5, H ₂] 7.47 [d, 1 H, <i>J</i> (HH) 7.5, H ₄] 7.70 (s, 1 H, H ₁) 6.9–7.3 (b, 15 H, PPh ₃)		 o-6b	0.57 [d, 3 H, <i>J</i> (PH) 7.1, Ir-Me] 1.06 [d, 9 H, <i>J</i> (PH) 9.8, PMe ₃] 1.53 [d, 15 H, <i>J</i> (PH) 1.7, C ₅ Me ₅] 6.75–7.05 (m, 3 H, H ₂ + H ₃ + H ₄) 7.38 [dd, 1 H, <i>J</i> (HH) = <i>J</i> (HF) = 5.9, H ₁]	
 p-5a	0.78 [d, 3 H, <i>J</i> (PH) 6.0, Ir-Me] 1.25 [d, <i>J</i> (PH) 1.8, C ₅ Me ₅] 7.15 [d, 2 H, <i>J</i> (HH) 8.1, H ₂] 7.38 [d, 2 H, <i>J</i> (HH) 8.1, H ₁] 6.9–7.3 (m, 15 H, PPh ₃)		 m-6b	0.53 [d, 3 H, <i>J</i> (PH) 6.8, Ir-Me] 0.91 [d, 9 H, <i>J</i> (PH) 9.8, PMe ₃] 1.44 [d, 15 H, <i>J</i> (PH) 1.7, C ₅ Me ₅] 7.18 [d, 1 H, <i>J</i> (HH) 7.6, H ₄] 6.75–7.05 (m, 2 H, H ₂ + H ₃) 7.30 [d, 1 H, <i>J</i> (FH) 11.7, H ₁]	
 10	1.32 [d, 15 H, <i>J</i> (PH) 1.9, C ₅ Me ₅] 6.9–7.6 (b m, 25 H, Ph + PPh ₃)	7.21	 p-6b	0.53 [d, 3 H, <i>J</i> (PH) 6.6, Ir-Me] 0.92 [d, 9 H, <i>J</i> (PH) 9.8, PMe ₃] 1.46 [d, 15 H, <i>J</i> (PH) 1.7, C ₅ Me ₅] 6.75–7.05 (m, 2 H, H ₂) 7.24 [dd, 2 H, <i>J</i> (HH) 6.8 <i>J</i> (FH) 6.6, H ₁]	

Table 1. (Continued)

	^1H	^{31}P		^1H	^{31}P
 <i>m,m'</i>-11	1.19 [d, 15 H, $J(\text{PH})$ 1.4, C_5Me_5] 6.67 [t, 2 H, $J(\text{HH})$ 5.0, H_3] 7.19 [d, 2 H, $J(\text{HH})$ 5.6, H_2] 7.42 [d, 2 H, $J(\text{HH})$ 5.6, H_4] 7.95 (s, 2 H, H_1) 6.9–7.3 (m, 15 H, PPh_3)		 <i>m</i>-7b	0.52 [d, 3 H, $J(\text{PH})$ 6.6, Ir–Me] –39.23 0.90 [d, 9 H, $J(\text{PH})$ 9.9, PMe_3] 1.43 [d, 15 H, $J(\text{PH})$ 1.8, C_5Me_5] 6.88 [t, 1 H, $J(\text{HH})$ 8.5, H_3] 7.14 [d, 1 H, $J(\text{HH})$ 8.8, H_2] 7.25 [d, 1 H, $J(\text{HH})$ 8.5, H_4] 7.58 (s, 1 H, H_1)	
 <i>m,p'</i>-11	1.16 [d, 15 H, $J(\text{PH})$ 1.2, C_5Me_5] 6.60 [t, 1 H, $J(\text{HH})$ 5.0, H_3] 7.02 [d, 1 H, $J(\text{HH})$ 4.8, H_4] 7.05 [d, 2 H, $J(\text{HH})$ 5.4, H_6] 7.18 [d, 1 H, $J(\text{HH})$ 5.4, H_2] 7.41 [d, 2 H, $J(\text{HH})$ 5.4, H_5] 7.96 (s, 1 H, H_1) 6.9–7.3 (m, 15 H, PPh_3)		 <i>p</i>-7b	0.50 [d, 3 H, $J(\text{PH})$ 6.9, Ir–Me] –39.40 0.90 [d, 9 H, $J(\text{PH})$ 9.6, PMe_3] 1.44 [d, 15 H, $J(\text{PH})$ 1.6, C_5Me_5] 7.13 [d, 2 H, $J(\text{HH})$ 8.5, H_2] 7.25 [d, 2 H, $J(\text{HH})$ 8.5, H_1]	
 <i>p,p'</i>-11	1.13 [d, 15 H, $J(\text{PH})$ 1.4, C_5Me_5] 7.01 [d, 4 H, $J(\text{HH})$ 5.0, H_1] 7.30 [d, 4 H, $J(\text{HH})$ 5.0, H_2] 6.9–7.3 (m, 15 H, PPh_3)		 <i>m</i>-8b	0.50 [d, 3 H, $J(\text{PH})$ 6.9, Ir–Me] –39.25 0.91 [d, 9 H, $J(\text{PH})$ 9.7, PMe_3] 1.42 [d, 15 H, $J(\text{PH})$ 1.8, C_5Me_5] 6.82 [t, 1 H, $J(\text{HH})$ 7.5, H_3] 7.25 [d, 1 H, $J(\text{HH})$ 7.5, H_2] 7.27 [d, 1 H, $J(\text{HH})$ 7.5, H_4] 7.73 (s, 1 H, H_1)	
 12	0.76 [d, 3 H, $J(\text{PH})$ 6.3, Ir–Me] 1.62 [d, 15 H, $J(\text{PH})$ 2.3, C_5Me_5] 6.85–7.25 (m, 10 H, PPh_2) 7.27–7.35 (m, 2 H, $\text{H}_1 + \text{H}_4$) 7.72 [dt, 2 H, $J(\text{HH})$ 9.5, $\text{H}_2 + \text{H}_3$]	–57.50	 <i>p</i>-8b	0.48 [d, 3 H, $J(\text{PH})$ 6.7, Ir–Me] –39.44 0.88 [d, 9 H, $J(\text{PH})$ 9.6, PMe_3] 1.43 [d, 15 H, $J(\text{PH})$ 1.7, C_5Me_5] 7.19 [d, 2 H, $J(\text{HH})$ 8.5, H_1] 7.30 [d, 2 H, $J(\text{HH})$ 8.5, H_2]	
 1b	0.43 [d, 6 H, $J(\text{PH})$ 5.7, Ir–Me] 1.04 [d, 9 H, $J(\text{PH})$ 9.5, PMe_3] 1.63 [d, 15 H, $J(\text{PH})$ 1.8, C_5Me_5]	–41.92	 <i>m</i>-9b	0.48 [d, 3 H, $J(\text{PH})$ 6.6, Ir–Me] 0.84 [d, 9 H, $J(\text{PH})$ 9.6, PMe_3] 1.35 [d, 15 H, $J(\text{PH})$ 1.8, C_5Me_5] 6.83 [t, 1 H, $J(\text{HH})$ 7.5, H_2] 7.54 [d, 1 H, $J(\text{HH})$ 7.5, H_4] 7.89 [d, 1 H, $J(\text{HH})$ 7.5, H_2] 8.43 (s, 1 H, H_1)	
 2b	0.62 [d, 3 H, $J(\text{PH})$ 6.8, Ir–Me] 0.97 [d, 9 H, $J(\text{PH})$ 9.5, PMe_3] 1.51 [d, 15 H, $J(\text{PH})$ 1.8, C_5Me_5] 7.1–7.25 (m, 3 H, $\text{H}_2 + \text{H}_3$) 7.48 [dd, 2 H, $J(\text{HH})$ 7.9, $J(\text{HH})$ 1.6, H_1]	–38.92	 <i>p</i>-9b	0.43 [d, 3 H, $J(\text{PH})$ 6.6, Ir–Me] 0.81 [d, 9 H, $J(\text{PH})$ 9.3, PMe_3] 1.37 [d, 15 H, $J(\text{PH})$ 1.8, C_5Me_5] 7.33 [d, 2 H, $J(\text{HH})$ 8.4, H_1] 7.89 [d, 2 H, $J(\text{HH})$ 8.4, H_2]	

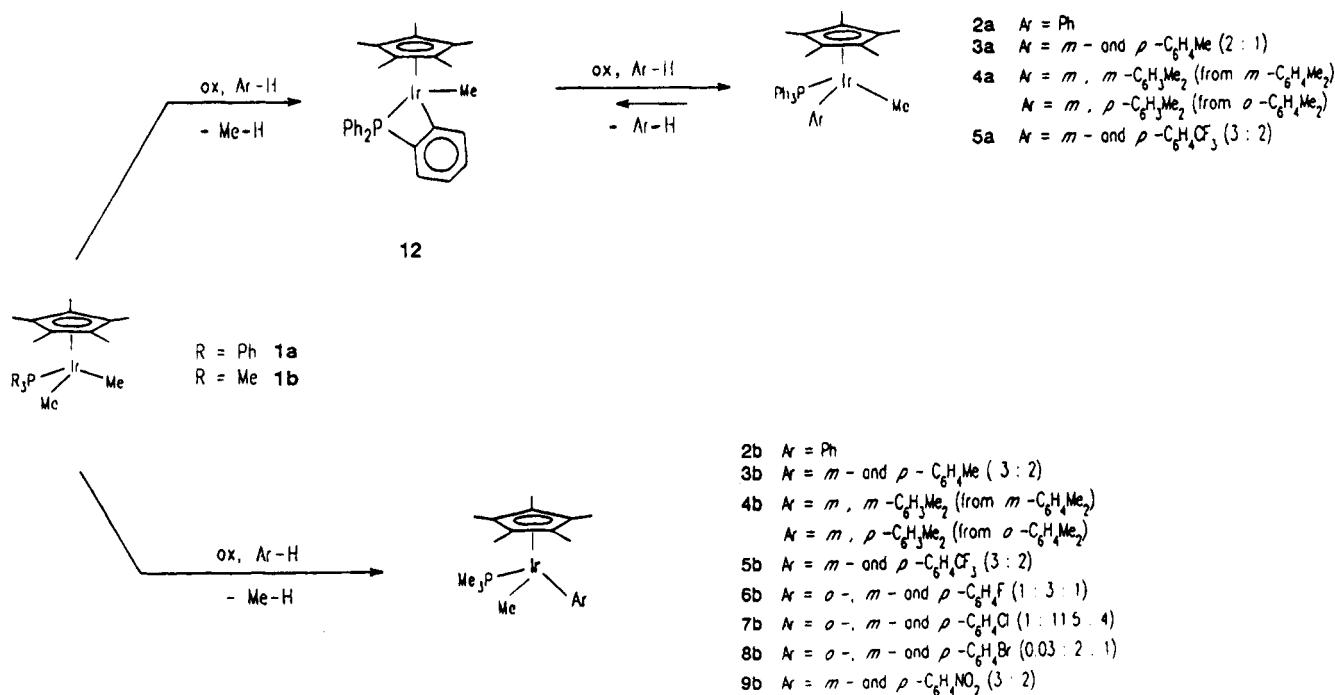
^a Spectra obtained in benzene-*d*₆; given as chemical shift (δ) [multiplicity, relative intensity, coupling (J in Hz), assignment]. ¹⁹F NMR, δ : ***m*-5b**, 7.70; ***p*-5b**, 8.52.

Section). As already noted for the thermolysis reactions of **1a**, in all cases the *ortho* positions do not react, presumably for steric reasons. So in toluene only the *meta* and *para* C–H bonds are activated with the *meta/para* ratio (2/1) corresponding to the statistical value, and in the case of xylenes only *o*- and *m*-xylene react to give respectively ***m,p***- and ***m,m***-**4a**. No evidence for benzylic C–H activation has been acquired. The equilibrium between the inter- and intramolecular activation product seems to depend on the number of reactive C–H bonds: the conversion of **12** into the intermolecular product is 75% in the reaction with toluene, 60% with *o*-xylene, 40% with *m*-xylene, and 0% with *p*-xylene. Unexpectedly, reaction of **1a** with trifluorotoluene (having almost identical steric requirements as toluene) only affords the intermolecular activation

product $\text{Cp}^*\text{Ir}(\text{PPh}_3)(\text{Me})(\text{C}_6\text{H}_4\text{CF}_3)$ (**5a**) as a (3/2) mixture of the *meta* and *para* isomers.

In order to study the potentiality of the reaction and to avoid complications due to orthometalation of the phosphine, we have examined the reactions of the complex $\text{Cp}^*\text{Ir}(\text{PMe}_3)_2\text{Me}$ (**1b**), which is expected to be more resistant to cyclometalation. In fact **1b** reacts with benzene in the presence of ferrocenium hexafluorophosphate under the same conditions given above to give (quantitatively, in 1 h) $\text{Cp}^*\text{Ir}(\text{PMe}_3)(\text{Me})(\text{Ph})$ (**2b**), which can be easily isolated by column chromatography followed by crystallization. When treated with benzene-*d*₆, a mixture of CH_4 and CH_3D is produced, the relative amounts being 2/3. This is a clear indication of two competitive patterns: a direct reaction between **1b** and benzene-*d*₆ and a ligand C–H activation to an unstable

Scheme 2

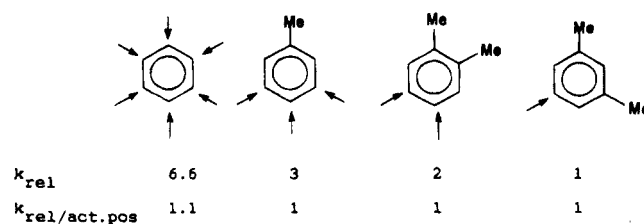


product, followed by fast reaction with benzene-*d*₆ to give **3b-d**₆. ²H NMR spectroscopy shows indeed the presence of deuterium on the pentamethylcyclopentadienyl ligand ($\delta = 3.98$) (in addition to the Ir-C₆D₅ resonances), thus giving evidence of this ligand as a source of hydrogen atoms. It has already been observed in the literature^{10c,d} that, in some C-H activation reactions by cyclopentadienylmetal derivatives, metalation of the Cp* ligand can occur to give a transient "tucked-in" derivative (see below). It is plausible that Cp* activation, in addition to direct orthometalation of the phosphine, is also operating in the case of **1a**. An estimate of the kinetic isotopic effect has also been made by reacting **1b** with benzene/benzene-*d*₆ mixtures in various proportions and evaluating the Ir-C₆H₅/Ir-C₆D₅ ratio by ¹H NMR spectroscopy: a rather moderate value of 2.2 was found for k_H/k_D .

The reaction works equally well with substituted arenes (Scheme 2), thus providing a facile route to the synthesis of methylaryliridium derivatives. In the case of toluene, a mixture of the *m*- and *p*-isomers Cp*Ir(PMe₃)(Me)(C₆H₄Me) (**3b**) is obtained in a 3/2 ratio, while in the case of xylenes, only Cp*Ir(PMe₃)(Me)(*m,p*-C₆H₃Me₂) (**4b**) is formed from *o*-xylene, Cp*Ir(PMe₃)(Me)(*m,m*-C₆H₃Me₂) (**4b**) from *m*-xylene, and nothing from *p*-xylene. Other monosubstituted arenes (fluorobenzene, chlorobenzene, bromobenzene, trifluorotoluene, nitrobenzene) react to give a mixture of the *m*- and *p*-isomers, their ratio being always close to the statistical value, independent of the electron-withdrawing or -releasing power of the group.

The kinetic selectivity of **1b** toward substituted arenes was also investigated. An ¹H NMR study of the reaction with benzene-*d*₆ or toluene-*d*₈ under pseudo-first-order conditions showed good first-order plots, although the rate constants are not very reproducible owing to the heterogeneity of the system. We therefore followed the reaction of equimolar mixtures of arenes, and assuming that the same first-order law is valid in all cases, we have derived the following relative scale of reactivity (the values of the relative kinetic constants are given

in parentheses): Ar-H (8.8) > Ar-F (4.4) > Ar-Me = Ar-Cl = Ar-Br (4) > Ar-CF₃ = ArNO₂ (1). All these data seem to exclude the influence of electronic factors in determining the selectivity of the reaction. The regiochemistry too does not seem to depend on electronic factors, since in the reactions with benzene, toluene, and xylenes the kinetic constants relative to the number of active positions of the arene are practically identical.



In order to exclude a thermodynamic control of the observed selectivity operating through scrambling reactions between the σ -bonded aryl group and free arene, the methyl aryl derivatives have been treated with benzene in the presence of the oxidant. Since in no case has the σ -aryl ligand been substituted by the phenyl group, we must conclude that the selectivity is kinetic indeed.

Other 1-electron oxidants have been tested as promoters for the activation of benzene by **1a** and **1b**. While Fe(acac)₃ and methylviologen dichloride do not give any reaction, AgBF₄ and Ph₃C⁺BF₄⁻ behave like ferrocenium hexafluorophosphate, giving **2b** from **1b** and a 15/85 mixture of **12** and **2a** from **1a** (the same equilibrium composition obtained with the ferrocenium cation).

With the aim of establishing if the above reactivity could be exhibited by other metal dialkyls, we have also studied the reactivity of related iridium(III) and rhodium(III) dialkyl derivatives, Cp*Ir(PPh₃)R₂ (R = CH₂-SiMe₃ (**13**); R₂ = CH₂SiMe₂CH₂ (**14**), Cp*Rh(PR'₃)Me₂ (R' = Ph (**15a**), Me (**15b**)), and Cp*Rh(PPh₃)R₂ (R = CH₂SiMe₃ (**16**); R₂ = CH₂CMe₃CH₂ (**17**)), with Cp₂Fe⁺-

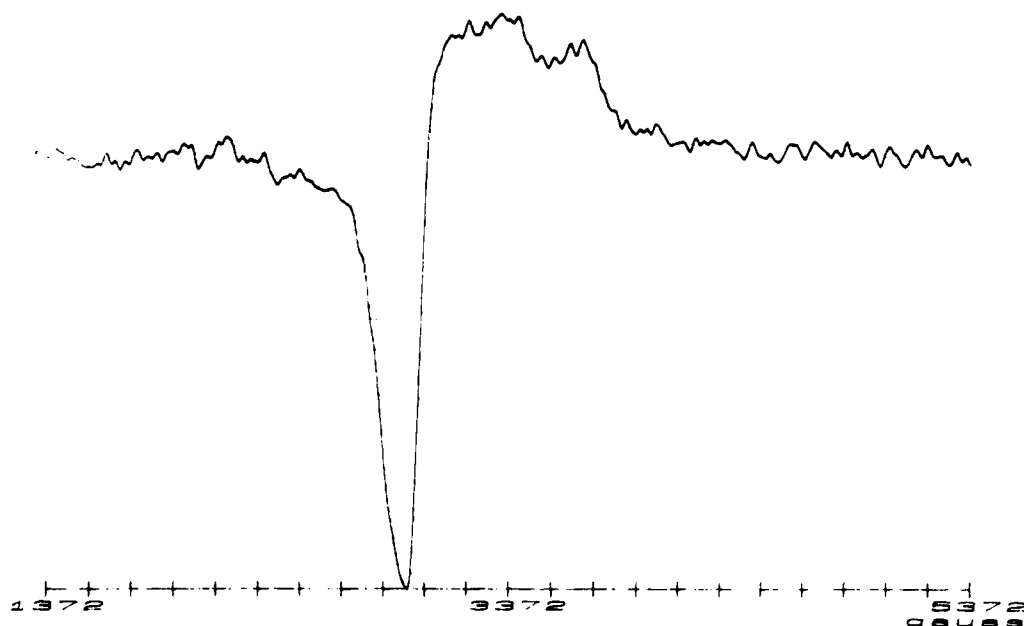


Figure 1. ESR spectrum at 120 K of the species obtained by reaction of **1a** with AgBF_4 in CH_2Cl_2 .

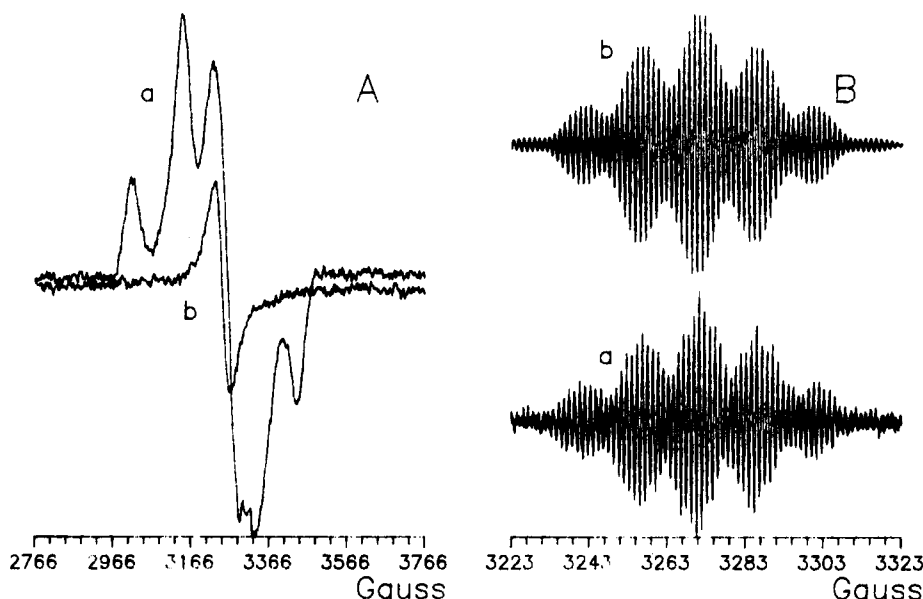


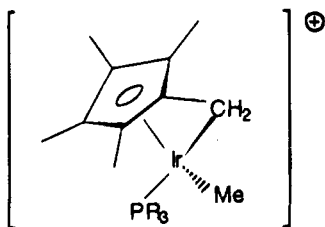
Figure 2. ESR spectra of the species obtained by reaction of **1b** with AgBF_4 in CH_2Cl_2 .

PF_6^- in benzene: we never observed activation of aromatic C-H bonds. The reaction leads to the almost stoichiometric oxidation (on the basis of the amounts of formed ferrocene) of the dialkyl complex, yielding a deep-red/deep-green gummy solid. Oxidation is accompanied by decomposition of the dialkyl groups, as shown by the formation of SiMe_4 and CH_4 in the case of complexes **13**, **14**, **16**, and **17** and of C_2H_6 and CH_4 in the case of rhodium compounds **15a** and **15b** (analogous results have been reported by Tilset¹⁰ for the oxidation of **15a** in CH_2Cl_2). We were unable to isolate the resulting organometallic products.

ESR Studies of the Chemical Oxidation of **1a, **1b**, and Related Iridium Dialkyls.** In order to acquire some mechanistic information on the above reactions, we initiated an ESR study of the oxidation of **1a** and **1b**. Preliminary experiments, carried out using various ferrocenium salts, revealed that the presence of iron(III) centers could mask the observation of spectra associated with the *in situ* generated iridium paramagnetic species, perhaps as a consequence of intermolecu-

lar spin-spin interactions. Moreover, because of the poor solubility of the cationic iridium oxidation products in arenes, we chose to use CH_2Cl_2 as the solvent. AgBF_4 in CH_2Cl_2 was conveniently used. Under these conditions, the oxidation of **1a** proceeds easily even at low temperature (120 K, solid state), generating a species **1a**⁺, the ESR spectrum of which ($g_\perp = 2.1720$; $g_\parallel = 1.8120$) is reported in Figure 1. Analogously, by oxidation of **1b** at 173 K an ESR-active species **1b**⁺ which gives rise to a single-line signal centered at $g_{\text{iso}} = 2.0090$ (Figure 2a) is obtained. When the sample is cooled to 82 K, the spectrum appears as the superposition of two sets of signals, each having three different g values (this could be due to the presence of two isomeric forms resulting from the existence of two different positions of the Cp ring with respect to the other ligands). Due to the lack of hyperfine structure, a detailed determination of the structure of the primary 1-electron-oxidation products **1a**⁺ and **1b**⁺ is not possible. Raising the temperature above 173 K causes the intensity of the above ESR patterns to decrease slowly in both cases

until, at 253 K, vigorous evolution of methane starts to occur and new spectra appear. The spectra of the two species are practically identical, but owing to the longer lifetime, only in the case of the cation radical deriving from **1b** is the spectrum ($\Delta H_{pp} = 0.8$ G) sufficiently intense to be satisfactorily compared to a computer-simulated one (Figure 2B(b)), which is consistent with a radical having a spin delocalization confined to two sets of two methyl groups ($a_H = 14.6$ G and $a_H = 2.7$ G), to the iridium atom ($a_{Ir} = 2.7$ G), and finally to one methylene group ($a_H = 1.35$ G). Furthermore, oxidation of $\text{Cp}^*\text{Ir}(\text{PMe}_3)(\text{CD}_3)_2$ **1b-d₆** gives a radical displaying almost the same spectrum, apart from a small decrease of the signal width. On this basis, we attribute to these radicals the "tucked-in"^{6c,d} structure



This is nicely consistent with the observed partial substitution of a hydrogen by a deuterium atom in the Cp^* ligand after the reaction of **1b** with benzene- d_6 and strongly supports the role of the "tucked-in" intermediate in the intramolecular mechanistic pathway of the arene activation reactions (see above). It is worthwhile to stress that, according to ESR evidence, the Cp^* methyl groups are metalated even in the case of **1a**, where chemical oxidation in dichloromethane eventually causes metalation of the triphenylphosphine ligand.

Similar experiments performed on the dialkyl derivatives **13** and **14** have shown the formation at low temperature (113 K, solid state) of the corresponding paramagnetic species **13⁺** ($g_{\perp} = 2.191$, $g_{\parallel} = 1.963$) and **14⁺** ($g_{\perp} = 1.9642$, $g_{\parallel} = 2.2101$). At 233 K the spectrum of **13⁺** appears as a single-line signal ($g = 2.139$). The signals slowly disappear when the temperature is raised, and no new signals are detected.

Electrochemical Oxidation of 1a, 1b, and Related Rhodium and Iridium Dialkyls. The cyclic voltammetric responses shown in Figure 3 give evidence for the different redox aptitudes of **1a** and **1b**, in dichloromethane solution, at ambient temperature.

Both complexes undergo an anodic process, which, in controlled-potential coulometry, consumes 1 electron/molecule; in the case of **1a**, the oxidation process displays features of chemical reversibility, whereas for **1b**, fast chemical complications follow the electron transfer.

Analysis¹⁷ of the cyclic voltammetric responses relative to **1a**, with the scan rate v varying from 0.02 to 20.48 V s^{-1} , shows that (i) the peak current ratio i_{pc}/i_{pa} is constantly equal to 1, (ii) the peak-to-peak separation, ΔE_p , progressively increases from 68 to 374 mV, and (iii) the current function $i_{pa}/v^{1/2}$ remains substantially constant. Taking into account that, under the same experimental conditions, the 1-electron oxidation of ferrocene displays a similar increase of ΔE_p with scan rate, one can conclude that the **1a/1a⁺** oxidation involves a chemically and electrochemically reversible 1-electron removal, at least in the short time scale of cyclic voltammetry [$t_{1/2}(\text{1a}^+) \approx 30$ s]. As a matter of

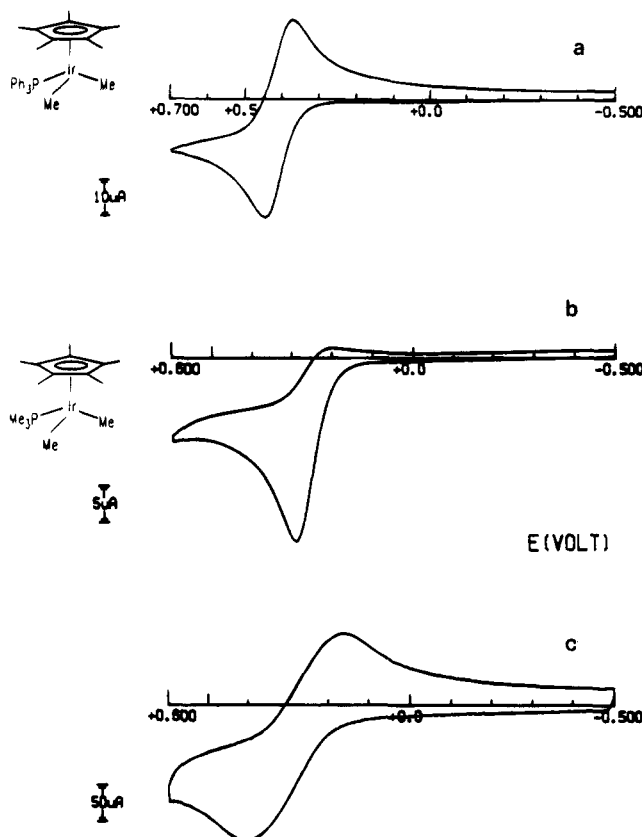


Figure 3. Cyclic voltammograms recorded at a platinum electrode on CH_2Cl_2 solutions containing $[\text{NBu}_4][\text{ClO}_4]$ (0.2 mol dm^{-3}) and (a) **1a** ($2.1 \times 10^{-3} \text{ mol dm}^{-3}$) or (b, c) **1b** ($1.5 \times 10^{-3} \text{ mol dm}^{-3}$). Scan rates: (a, b) 0.2 V s^{-1} ; (c) 20.48 V s^{-1} .

fact, in the longer times of macroelectrolysis at ambient temperature, full decomposition of the exhaustively electrogenerated cation **1a⁺** occurs. During the test, the starting pale yellow solution first turns red-violet and then degrades slowly to yellow. Quite similar results have been obtained by Tilset.^{13b} At the end of the electrolysis, cyclic voltammetry shows no more evidence of the presence of the **1a/1a⁺** couple. Nevertheless, by performing the macroelectrolysis test at -20°C , we see that the red-violet color of the 1-electron-oxidized species **1a⁺** persists in solution for a time sufficiently long to allow its ESR spectrum to be recorded (see below). It has to be noted that the initial red-violet color was also obtained at the first stages of the above described chemical oxidation.

As for the analysis of the cyclic voltammetric responses of **1b** at increasing scan rates, the most significant parameter, the i_{pc}/i_{pa} ratio, progressively increases from 0.26 at 0.2 V s^{-1} to 1 at 20.48 V s^{-1} . This allows us¹⁷ to assign a lifetime ($t_{1/2}$) of about 0.05 s to the primarily electrogenerated monocation **1b⁺**.

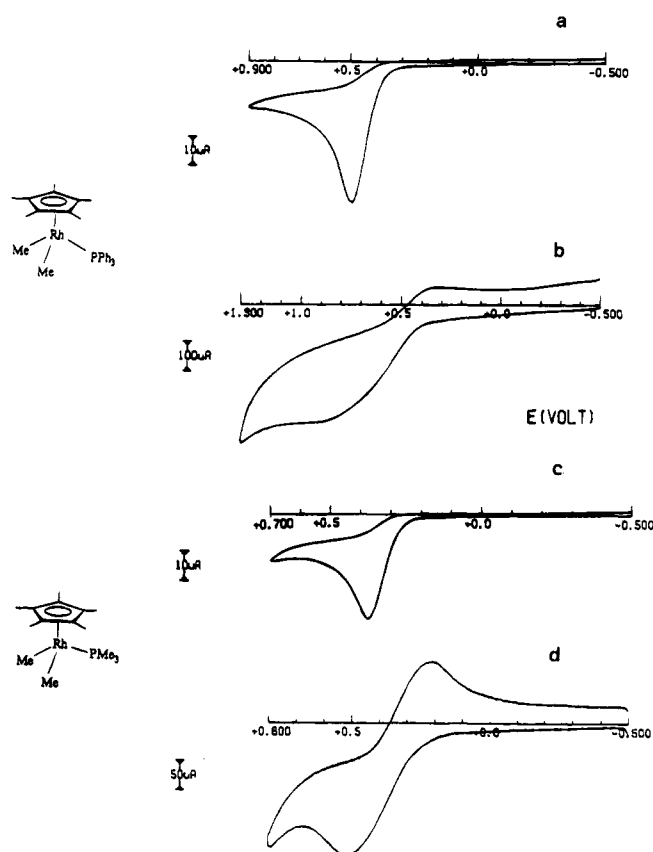
Table 2 summarizes the redox potentials for the electron removals exhibited by the complexes here studied.

Interestingly, the presence of the more basic PMe_3 ligand in **1b** favors the thermodynamic access to the corresponding Ir(IV) cation, which however is kinetically more labile. A similar difference in kinetic stability of the 1-electron-oxidized species holds for the iridium

(17) Brown, E. R.; Sandifer, J. In *Physical Methods of Chemistry. Electrochemical Methods*; Rossiter, B. W., Hamilton, J. F., Eds.; Wiley: New York, 1986; Vol. 2, Chapter 4.

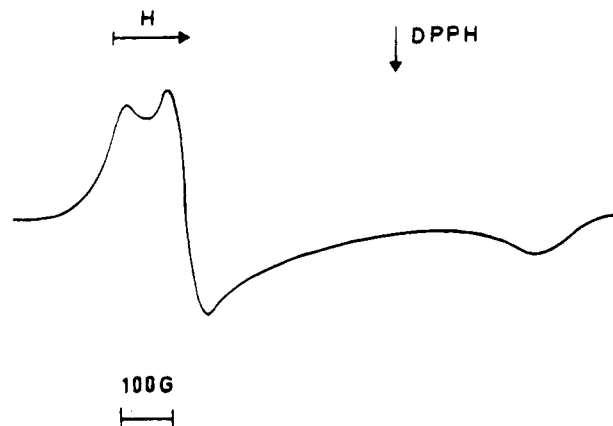
Table 2. Electrochemical Characteristics of the Oxidation Processes of the Iridium and Rhodium Complexes

com- plex	E^{ox} (0/+) (V, vs SCE)	E_p (mV)	i_{pc}/i_{pa}^a	$t_{1/2}$ (mono- cation) ^b (s)	solvent
1a	+0.41	82 ^a	1	≥ 30	CH ₂ Cl ₂
	+0.42 ^c				CH ₂ Cl ₂
	+0.64	108 ^a	1	≥ 30	THF
	+0.41 ^c				MeCN
1b	+0.28	114 ^d	0.26	≈ 0.05	CH ₂ Cl ₂
12	+0.51	116 ^d	0.21	≈ 0.04	CH ₂ Cl ₂
13	+0.31	80 ^a	0.55	≈ 1	CH ₂ Cl ₂
	+0.54	170 ^b	0.50	≈ 1	THF
14	+0.09	70 ^a	1	≥ 30	CH ₂ Cl ₂
15a	+0.49 ^{a,e}		<i>f</i>	≤ 0.01	CH ₂ Cl ₂
	+0.5 ^c				MeCN/CH ₂ Cl ₂
15b	+0.36	126 ^d	0.34	≈ 0.2	CH ₂ Cl ₂
16	+0.34 ^{a,e}		<i>f</i>	≤ 0.01	CH ₂ Cl ₂
17	+0.14 ^{a,e}		<i>f</i>	≤ 0.01	CH ₂ Cl ₂

^a Measured at 0.2 V s⁻¹. ^b Cyclic voltammetric time scale.^c Reference 13b. ^d Measured at 1.0 V s⁻¹. ^e Peak potential value.^f No associated peak in the reverse scan.**Figure 4.** Cyclic voltammograms recorded at a platinum electrode on CH₂Cl₂ solutions containing [NBu₄][ClO₄] (0.2 mol dm⁻³) and (a, b) **15a** (2.1 × 10⁻³ mol dm⁻³) or (c, d) **15b** (1.7 × 10⁻³ mol dm⁻³). Scan rates: (a, c) 0.2 V s⁻¹; (b) 51.20 V s⁻¹; (d) 20.48 V s⁻¹.

dialkyls **13** and **14**. As a matter of fact, the cyclic voltammogram of **14** shows features of chemical reversibility, whereas that of **13** shows evidence of relatively fast complications following the electron removal.

Nevertheless, the most dramatic difference in redox properties is found between iridium and rhodium analogues. As an example, Figure 4 shows the cyclic voltammetric behavior of the rhodium dimethyl complexes **15a** and **15b**, analogues of the iridium complexes **1a** and **1b**. As illustrated, the 1-electron oxidation is again coupled to fast chemical complications, but in this case, the presence of the electron-donating PMe₃ ligand

**Figure 5.** X-band ESR spectrum of the electrogenerated monocation [**1a**]⁺ in CH₂Cl₂ solution at *T* = 100 K.

favors both thermodynamically and kinetically the formation of the monocation.

Analogously, complex **16**, the rhodium congener of **13**, and complex **17** exhibit a response qualitatively similar to that of **15a**.

An interesting question arises from the fact that we were unable to electrochemically induce the chemically induced catalytic conversion of **1a** to **12** via loss of methane. In fact, in dichloromethane solution, **12** undergoes a 1-electron oxidation complicated by subsequent chemical reactions at potential values only slightly more anodic than that for **1a** ($\Delta E \approx 0.1$ V). This means that the driving force of the expected catalytic process should be rather low.^{1c} Nevertheless, even with the macroelectrolysis test performed at potential values corresponding to the rising part of the wave of **1a** (0.33 V ≤ *E*_w ≤ 0.40 V), in order to avoid the concomitant oxidation of the possibly electrogenerated species **12**, 1 electron/molecule is slowly consumed and the resulting solution does not exhibit any more significant redox properties. These electrochemical results prelude the fact that chemical and electrochemical oxidations follow different pathways. This was confirmed by the coupled electrochemical/ESR measurements.

ESR Characterization of the Electrogenerated Iridium(IV) Species 1a⁺, 13⁺, and 14⁺. Figure 5 shows the liquid nitrogen (100 K) X-band ESR spectrum of the monocation **1a**⁺, obtained by macroelectrolysis in CH₂Cl₂ solution at 253 K. The sample was withdrawn at the first stages of electrolysis (0.3 electron/molecule).

The anisotropic signal displays a well-resolved spectral pattern with orthorhombic symmetry, which can be suitably interpreted in terms of a *S* = 1/2 spin Hamiltonian. The relevant parameters have been evaluated by computer-simulated line shape analysis and are reported in Table 3.⁴

These glassy-solution parameters are characteristic of significant orbital contribution and are evidence for the metal-in nature of the *S* = 1/2 unpaired electron. There is no evidence for hyperfine (hpf) couplings of the unpaired electron with the magnetically active ¹⁹¹Ir and ¹⁹³Ir nuclei (*I* = 3/2), as well as for superhyperfine (shpf) coupling with the ³¹P nucleus (*I* = 1/2), probably because of the relatively large overall linewidth which overlaps any less separated hpf and shpf signals.¹⁸

When the temperature is raised, the signal rapidly drops out at the glassy/liquid phase transition, but upon

Table 3. X-Band ESR Parameters of the Electrogenerated Iridium(IV) Species in CH₂Cl₂ Solution

species	100 K				300 K	
	g_i	g_m	g_h	$\langle g \rangle$	g_{iso}	ΔH (G ^a)
[1a] ⁺	2.387	2.315	1.846	2.183		
[13] ⁺	2.326	2.239	1.943	2.169	2.015 ^d	160 ^a
[14] ⁺	2.160 ^b	2.011 ^c		2.110	2.111	80

^a ± 5 G. ^b \perp absorption. ^c \parallel absorption. ^d $g_{averaged} \pm 0.008$. $g_i \pm 0.004$.

freezing again, the starting absorption signal is restored. This reversible temperature dependence is highly indicative of the stability of the electrogenerated 1a⁺ complex while the corresponding spectral features give ESR evidence that active molecular distortions around the paramagnetic metal center are present, particularly under fast-motion conditions.

The paramagnetic cation 13⁺ displays a liquid-nitrogen X-band ESR spectrum similar to that of 1a⁺, with a large metal-in character signal (although of slightly reduced rhombic symmetry) and a significant orbital contribution. The relevant parameters are reported in Table 3. When the temperature is raised, the overall anisotropic line shape rapidly loses its rhombic pattern before the glassy/liquid phase transition, displaying a large, unresolved signal at $T > 180$ K (at 300 K, $\Delta H = 160$ G and $g_{av} = 2.015$). Again line shape analysis does not give evidence of hpf or shpf splittings because of the broad absorption pattern.

Finally, the monocation 14⁺ shows some interesting differences in terms of line shape analysis, at both liquid-nitrogen and room temperatures. Figure 6a shows the relevant X-band ESR spectrum recorded at 100 K.

The well-shaped axial parameters ($g_{\perp} > g_{\parallel}$) can be interpreted in terms of a $S = 1/2$ spin Hamiltonian and are indicative of an arrangement around the metal-centered unpaired electron more symmetrical than the previous rhombic ones. The corresponding computed spectrum is shown in Figure 6b, and the relevant parameters are reported in Table 3.

As illustrated in Figure 6c, when the temperature is raised, the line shape evolves to a single, relatively narrow unresolved isotropic signal centered at $g_{iso} = 2.111$, which displays a significant reduction of the spectral intensity, probably as a consequence of the chemical instability of the monocation. Once again, the actual large isotropic absorption pattern ($\Delta H = 80$ G) likely does not permit the detection of the magnetic couplings with the ¹⁹¹Ir, ¹⁹³Ir, and ³¹P nuclei. On the other hand, the peak-to-peak separation (ΔH) at 300 K, narrower than that of 13⁺, is indicative of longer electron spin relaxation times, in agreement with a more symmetric arrangement of the overall molecular framework around the unpaired electron.¹⁸ Thus the bulk of evidence shows that all the above electrochemically generated cations are metal-centered paramagnetic species and do not evolve to the AgBF₄-generated radicals.

Conclusions

The large increase in the reactivity toward arenes that the dimethyl complexes 1a and 1b exhibit in the presence of catalytic amounts of oxidants places the C–H activation reaction here described among the

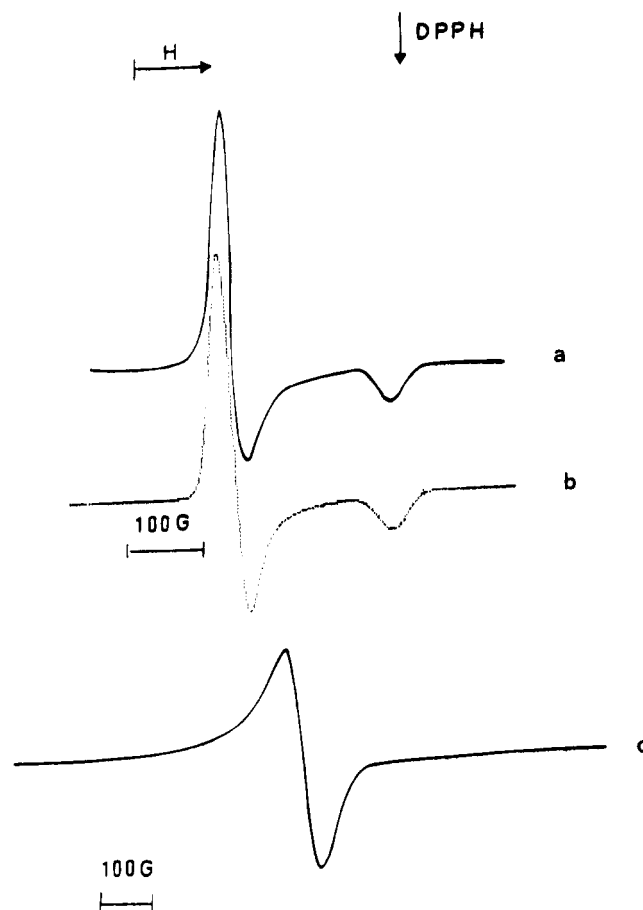
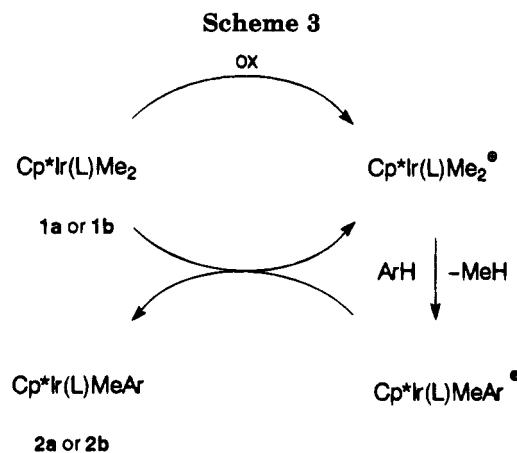


Figure 6. X-band ESR spectra of [14]⁺ in CH₂Cl₂ solution: (a) experimental and (b) simulated spectra at $T = 100$ K; (c) experimental spectrum at $T = 300$ K.



restricted number of electron transfer chain (ETC) catalyzed organometallic reactions.^{1b,c} According to this mechanistic scheme, the iridium species Cp*Ir(L)Me₂⁺ (L = PPh₃, PMe₃), deriving from a 1-electron oxidation of 1a or 1b, reacts rapidly with arenes to yield a cationic iridium derivative; this in turn oxidizes 1a or 1b and gives rise to the final methyl aryl compound 2a or 2b (Scheme 3).

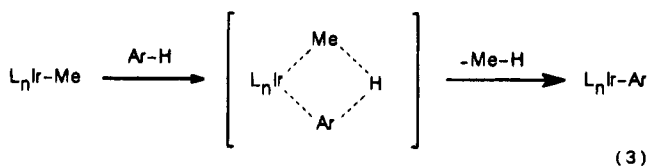
The cross-ET propagation step should probably be only slightly exergonic (and then rather slow) since the methyl ligand is just a bit more electron-releasing than an aryl one. As a consequence, the reactions are not very fast if compared with other more exergonic ETC reactions reported in the literature.¹ Fortunately, side reactions, a serious problem in ETC catalysis, do not seem to be too important in our cases.

Unfortunately electrochemical studies, which are generally quite informative about ETC reactions, are not very helpful in this case in supporting the reliability of such scheme; actually voltammetric techniques in CH_2Cl_2 show that $\mathbf{1a}^+$ does not convert to the orthometalated complex $\mathbf{12}$ as happens in the chemically induced reaction of $\mathbf{1a}$ in dichloromethane.

On the other hand, the radicals generated by Ag^+ oxidation of $\mathbf{1a}$ and $\mathbf{1b}$, which are best described in terms of a "tucked-in" structure (see above), should be mechanistically significant, also on the basis of the results obtained from the reaction of $\mathbf{1b}$ with deuterated benzene. In the ESR experiments carried out in the absence of aromatics, the intramolecular pattern obviously becomes the only one operative, and thus only the "tucked-in" radical is observed. The formation of this radical may reflect an electron-transfer mechanism, which substantially proceeds through the Cp^* ligand. Thus the bulk of evidence strongly supports the idea that chemical oxidation proceeds through a Cp^* -mediated inner-sphere mechanism, whereas the electrochemical oxidation involves the common outer-sphere mechanism.¹⁹ This would easily explain the different fate of the electrochemically and chemically generated species, which is known to depend in some cases on the nature of the oxidant.²⁰ Therefore it is possible that activation of arenes by these systems proceeds via two different intermediates, the "tucked-in" radical along the intramolecular pathway and another cationic derivative, perhaps the iridium(IV) cation, along the bimolecular route. The reason of the increased reactivity of the Cp^* -centered radical species obtained from chemical oxidation probably lies in the release of energy from the strained "tucked-in" intermediate which triggers the activation of the arene C–H bond. Instead the reactivity of the iridium(IV) system could most probably be related to the overcoming of the energy restrictions imposed by the saturated electron configuration in $\mathbf{1a}$ or $\mathbf{1b}$,^{1e,f} which prevent arene coordination. Alternatively, the access of arene to the iridium center can be thermally achieved by inducing the release of the phosphine ligand from $\mathbf{1a}$, and this easily explains the absence of the orthometalated product in the reaction mixture.

As for the mechanism of the aromatic C–H activation, we are inclined to disregard the oxidative addition pattern (quite common for late d transition metals and particularly for the iridium d^8 systems). The high oxidation state and some formal analogies are rather reminiscent of the " σ -bond metathesis" reactions, which have been described for early d transition metal systems. Moreover the following features are similar for the two systems: (i) the reaction is almost insensitive to the electron-donating or -attracting properties of the substituent on the arene but depends substantially on the number of arene reactive sites; (ii) the ratio (close to 2/1) of the *meta* vs *para* attack is almost purely statistic; (iii) the isotopic effect of the reaction with benzene ($k_{\text{H}}/k_{\text{D}} = 2.2$) implies a moderate but significant involvement of the cleavage of the C–H bond in the transition state of the slow step; (iv) the rate is well described by a first-order equation, which reflects two competitive pathways (intra- and intermolecular).

These features are consistent with the hypothesis of a concerted mechanism based on the formation of a four-center transition state as proposed for the " σ -bond metathesis" of C–H and M–C bonds by scandocene systems (eq 3).⁶



There is however a striking difference between the two systems, and this is the lack of reactivity toward nonaromatic C–H bonds. At the moment, we ignore whether this is just because of the poor solubility of the oxidant in aliphatic hydrocarbons or because of the intrinsic inactivity of the system. However it must be remembered that, in the reactions between arenes and the iridium dimethyl derivatives $\mathbf{1a}$ and $\mathbf{1b}$, the C–H bonds of the pentamethylcyclopentadienyl methyls are also activated to give a transient "tucked-in" intermediate. This suggests that even alkane activation may occur, but this could be masked by a rapid equilibration with other thermodynamically more favored reactions. Work is in progress in order to verify these ideas.

Experimental Section

General Procedures. The reactions and manipulation of organometallics were carried out under dinitrogen or argon, using standard techniques. The solvents were dried and distilled prior to use. The compounds $\text{Cp}^*\text{Ir}(\text{PPh}_3)\text{Cl}_2$,²¹ $\text{Cp}^*\text{Ir}(\text{PMe}_3)\text{Cl}_2$,²² $\text{Cp}^*\text{Ir}(\text{PMe}_3)\text{MeCl}$,²³ $\text{Cp}^*\text{Rh}(\text{PPh}_3)\text{Me}_2$,²¹ $\text{Cp}^*\text{Ir}(\text{PPh}_3)(\text{CH}_2\text{SiMe}_3)_2$,²⁴ $\text{Cp}^*\text{Ir}(\text{CH}_2\text{SiMe}_2\text{CH}_2)(\text{PPh}_3)_2$,²⁴ $\text{Cp}^*\text{Rh}(\text{PPh}_3)(\text{CH}_2\text{SiMe}_3)_2$,²⁴ $\text{Cp}^*\text{Rh}(\text{CH}_2\text{CMe}_2\text{CH}_2)(\text{PPh}_3)_2$,²⁴ and $\text{Cp}_2\text{Fe}^+\text{PF}_6^-$ ²⁵ were prepared according to literature procedures. AgBF_4 , $\text{Ph}_3\text{C}^+\text{BF}_4^-$, and methylviologen dichloride were Aldrich products. The ^1H NMR spectra were recorded using Varian Gemini 200 and VXR 300 spectrometers, operating respectively at 200 and 300 MHz. The ^1H NMR chemical shifts were referenced to residual protiated solvent as follows: benzene- d_6 , $\delta = 7.15$; dichloromethane- d_2 , $\delta = 5.32$. The ^{19}F , ^{31}P , and ^2H spectra were recorded on the VXR 300 instrument at 282, 121, and 46 MHz, respectively; the ^{19}F chemical shifts were referred to CFCl_3 as external standard, the ^{31}P chemical shifts to H_3PO_4 (external standard), and the ^2H data to benzene- d_6 (external standard). The 2D NOESY spectra were recorded in the phase-sensitive mode on the Varian VXR 300 spectrometer, and the temperature was controlled to $\pm 0.1^\circ\text{C}$. A spectral width of about 3000 Hz was used in both ω_1 and ω_2 dimensions, and the mixing time was 800 ms. The pulse delay was maintained at 10 s; 512 hypercomplex increments of 8 scans and 2K data points each were collected. The data matrix was zero-filled at $2\text{K} \times 2\text{K}$ and multiplied by a shifted Gaussian function in both dimensions. The monodimensional $^1\text{H}\{^1\text{H}\}$ NOE experiments were performed in the difference mode. The decoupler was placed at the required frequency to saturate the proton of interest. The decoupling power was the minimum required to saturate the spin. A waiting time of 10

(21) Kang, J. W.; Moseley, K.; Maitlis, P. M. *J. Am. Chem. Soc.* **1969**, 91, 5970.

(22) Isobe, K.; Bailey, P. M.; Maitlis, P. M. *J. Chem. Soc., Dalton Trans.* **1981**, 2003.

(23) Buchanan, J. M.; Stryker, J. M.; Bergman, R. G. *J. Am. Chem. Soc.* **1986**, 108, 1537.

(24) Andreucci, L.; Diversi, P.; Ingrosso, G.; Lucherini, A.; Marchetti, F.; Adovasio, V.; Nardelli, M. *J. Chem. Soc., Dalton Trans.* **1986**, 477.

(25) Brauer, G. *Handbuch der Präparativen Anorganischen Chemie*; Ferdinand Enke Verlag: Stuttgart, Germany, 1981; p 1845.

(19) *Electron-Transfer and Electrochemical Reactions; Photochemical and Other Energized Reactions*; Zuckerman, J. J., Ed.; Inorganic Reactions and Methods, Vol. 15; VCH Publishers: New York, 1986.

(20) Kochi, J. K. *Angew. Chem., Int. Ed. Engl.* **1988**, 27, 1227.

s was used. ESR spectra for the chemical oxidation reactions were obtained by using an EPR Varian E 112 instrument equipped with a Varian E 257 for temperature control. The spectrometer was interfaced to an AST Premium 486/25 by means of a data acquisition system consisting of an acquisition board capable of acquiring up to 500 000 12-bit samples/s, including 32-bit add-to memory, thus giving on-line signal averaging and a software package specially designed for ESR experiments.²⁶ Materials and methods for electrochemistry and EPR spectroscopy of the electrogenerated species have been described elsewhere.²⁷ All potential values are referred to the saturated calomel electrode (SCE). Under the present experimental conditions, the 1-electron oxidation of ferrocene occurs at $E^{\circ} = +0.45$ V in CH_2Cl_2 and at $E^{\circ} = +0.54$ V in THF solutions. X-band EPR spectra at $T = 100$ K and at room temperature were computed by the SIM14a computer simulation program.²⁸ Elemental analyses were performed by the Laboratorio di Microanalisi of the Istituto di Chimica Organica, Facoltà di Farmacia, University of Pisa.

Cp*Ir(PPh₃)Me₂ (1a). A suspension of Cp*Ir(PPh₃)Cl₂ (1 g, 1.55 mmol) in pentane (20 mL) was treated with MeMgI (120 mL of a 0.335 M solution in diethyl ether, 40 mmol) at room temperature for 20 h. 1,4-Dioxane (3.5 mL) was added and the suspension stirred for further 5 h. The reaction mixture was hydrolyzed with water, and the pentane extracts were collected and dried. The product was purified by column chromatography on alumina using pentane/ether (1/1) as the eluant to give 0.88 g (94% yield) of **1a**, which was crystallized from pentane to give pale-yellow crystals having the same ¹H NMR spectrum as that of the compound prepared by a different route.²⁹

Cp*Ir(PMe₃)Me₂ (1b). MeMgI (90 mL of a 0.30 M diethyl ether solution, 27 mmol) was added slowly to Cp*Ir(PMe₃)Cl₂ (1 g, 2.1 mmol). The mixture was stirred for 24 h at room temperature and then evaporated to dryness, extracted with pentane, and treated with 1,4-dioxane (1 mL). After removal of the magnesium salts, the resulting solution was evaporated to dryness. The residue was extracted with pentane and hydrolyzed with water at 0 °C. The organic extracts were dried over sodium sulfate and evaporated to dryness under vacuum, to give pale-yellow crystals (0.7 g, 77%) of **1a** having the same properties as those of a sample prepared by an alternative route.²³

Cp*Ir(PMe₃)Me-d₆ (1b-d₆). According to the above procedure, Cp*Ir(PMe₃)Cl₂ (0.15 g, 0.32 mmol) in pentane (5 mL) was reacted with (Me-d₆)MgI (2.5 mL of a 1 M solution in diethyl ether, 2.5 mmol) for 9 h at room temperature to give 0.1 g of **1b-d₆** (72%) having the same ¹H NMR spectrum as that reported in the literature for an authentic sample.²³

Cp*Rh(PMe₃)Me₂ (15b). Cp*Rh(PMe₃)Cl₂ (0.39 g, 1 mmol) in pentane (15 mL) was treated with MeMgI (10 mL of a 0.33 M solution in diethyl ether, 3.3 mmol). After 16 h, the mixture was evaporated to dryness, extracted with pentane, and hydrolyzed with water. The pentane extracts were dried over sodium sulfate and concentrated. By crystallization at -30 °C yellow crystals of **15b** were obtained (0.24 g, 70%). Anal. Calcd for C₁₅H₃₀PRh: C, 52.31; H, 8.79; P, 9.00. Found: C, 52.15; H, 8.76; P, 8.70. ¹H NMR (benzene-d₆): δ 0.15 (6 H, dd, $J(\text{PH})$ 5.3 Hz, $J(\text{RhH})$ 2.5 Hz, Rh-Me) 0.89 (9 H, dd, $J(\text{PH})$ 9.2 Hz, $J(\text{RhH})$ 1.0 Hz, PMe₃), 1.63 (15 H, d, $J(\text{PH})$ 2.3 Hz, Cp*).

Cp*Ir(PPh₃)(Me)(Ph) (2a). A suspension of Cp*Ir(PPh₃)Cl₂ (0.21 g, 0.3 mmol) was reacted with MeMgI (20 mL of a 0.3 M solution in diethyl ether, 6 mmol). After 40 h, the suspension was hydrolyzed, and the collected pentane extracts were dried over sodium sulfate. The crude product was transferred to the top of a chromatography column (alumina).

Benzene eluted a band of the pure halomethyl derivative. ¹H NMR (benzene-d₆): δ 1.36 (15 H, d, $J(\text{PH})$ 1.94 Hz, Cp*), 1.57 (3 H, d, $J(\text{PH})$ 6.35, Ir-Me), 7.02 (9 H, m, Ph), 7.72 (6 H, m, Ph). This product was added to pentane (5 mL) and treated with PhMgBr (1 mL of a 1.7 M solution in diethyl ether, 1.7 mmol). After 2 h, 1,4-dioxane was added and the reaction mixture stirred for 36 h. After hydrolysis and extraction with pentane, a solid residue was obtained that was chromatographed on alumina with pentane/benzene (2/1) to give a pale-yellow band from which green-yellow crystals of **2a** (50% yield) were obtained. Anal. Calcd for C₃₃H₃₈IrP: C, 61.65; H, 5.62; P, 4.54. Found: C, 61.61; H, 5.60; P, 4.49.

Cp*Ir(PPh₃)Ph₂ (10). A suspension of Cp*Ir(PPh₃)Cl₂ (0.17 g, 0.26 mmol) in pentane (5 mL) was treated with PhMgBr (2.5 mL of a 1.7 M solution in diethyl ether, 4.25 mmol), and the mixture was stirred for 2 h. 1,4-Dioxane was added, and the suspension was stirred for 24 h. After the usual workup and column chromatography on alumina by eluting with pentane/ether, a central yellow band was collected, which was evaporated to dryness and then extracted with pentane. The residue was crystallized from pentane/ether to give yellow crystals of **10** (20% yield). Anal. Calcd for C₄₀H₄₀IrP: C, 64.58; H, 5.42; P, 4.16. Found: C, 64.47; H, 5.41; P, 4.05.

Cp*Ir(PPh₃)(Me)(*m*-C₆H₄Me) (m-3a). A suspension of Cp*Ir(PPh₃)Cl₂ (0.31 g, 0.45 mmol) in diethyl ether (15 mL) was treated with (*m*-C₆H₄Me)MgBr (1.0 M solution in diethyl ether, 1.15 mmol), and the mixture was stirred at room temperature for 40 h. The mixture was then evaporated to dryness under vacuum, and the solid residue was hydrolyzed at 0 °C with water, extracted with ether, and chromatographed on a column of alumina. Pentane/benzene (1/1) eluted a yellow band which by crystallization from pentane gave orange crystals of Cp*Ir(PPh₃)(Br)(*m*-C₆H₄Me) (0.19 g, 55% yield). Anal. Calcd for C₃₅H₃₇BrIrP: C, 55.26; H, 4.90; Br, 10.50. Found: C, 55.41; H, 4.82; Br, 10.01. ¹H NMR (benzene-d₆): δ 1.26 (15 H, d, $J(\text{HP})$ 1.9 Hz, Cp*), 2.17 (3 H, s, C₆H₄Me), 6.80–7.35 (18 H, b m, PPh₃, C₆H₄Me), 7.90 (1 H, b s, C₆H₄Me). These crystals were suspended in pentane (1 mL) and treated with MeMgI (4 mL of a 0.3 M solution in diethyl ether, 1.2 mmol). After 14 h at room temperature, the mixture was evaporated to dryness, extracted with pentane, and hydrolyzed with water. The organic phase was dried over Na₂SO₄ and chromatographed on an alumina column to give yellow crystals (0.1 g, 57%). Anal. Calcd for C₃₆H₄₀IrP: C, 62.13; H, 5.79. Found: C, 62.26; H, 5.86.

Cp*Ir(PPh₃)(Me)(*p*-C₆H₄Me) (p-3a). Cp*Ir(PPh₃)Cl₂ (0.33 g, 0.48 mmol) was reacted with MeMgI (30 mL of a 0.3 M solution in diethyl ether, 9 mmol) by the procedure described for **2a** to give the monomethyl derivative, which was suspended in pentane (7 mL) and treated with Mg(*p*-tolyl)Br (3 mL of a 1 M solution in diethyl ether, 3 mmol). After 16 h, 1 mL of 1,4-dioxane was added, and the mixture was stirred for further 24 h. The solvent was removed under vacuum, and the residue was taken up in pentane and hydrolyzed. The combined pentane/ether (5/1) extracts were dried over sodium sulfate and evaporated to dryness. The crude yellow solid was dissolved in a minimum amount of benzene. Column chromatography on alumina, eluting with pentane, gave yellow-brown crystals of **p-3a** (0.16 g, 47%). Anal. Calcd for C₃₆H₄₀IrP: C, 62.13; H, 5.79. Found: C, 61.96; H, 5.75.

Cp*Ir(PMe₃)(Me)(*p*-C₆H₄Me) (p-3b). Cp*Ir(PMe₃)(Me)(Cl) (0.065 g) in diethyl ether (2 mL) was treated with (*p*-C₆H₄Me)MgBr (1 mL of a 1 M solution in diethyl ether, 1 mmol) for 20 h. The suspension was evaporated to dryness and extracted with pentane. The pentane extracts were hydrolyzed, and the organic layer was dried over sodium sulfate and evaporated to dryness to give **p-3b** as a yellow solid (42 mg, 57%). Anal. Calcd for C₂₁H₃₄IrP: C, 49.49; H, 6.72. Found: C, 49.28; H, 6.70.

Cp*Ir(PMe₃)(Me)(*m*-C₆H₄Me) (m-3b). According to the above procedure, Cp*Ir(PMe₃)(Me)(Cl) (0.066 g, 0.15 mmol) was reacted with (*m*-C₆H₄Me)MgBr (1 mL of a 1 M solution

(26) Ambrosetti, R.; Ricci, D. *Rev. Sci. Instrum.* **1991**, 62, 2281; ESR-ENDOR, ICQEM-CNR, 1992.

(27) Osella, D.; Ravera, M.; Nervi, C.; Housecroft, C. E.; Raithby, P. R.; Zanello, P.; Laschi, F. *Organometallics* **1991**, 10, 3253.

(28) Lozos, J. P.; Hoffman, B. M.; Franz, C. G. *QCPE* **1973**, 11, 243.

(29) Glueck, D. S.; Bergman, R. G. *Organometallics* **1991**, 10, 1479.

in diethyl ether, 1 mmol) to give after crystallization from pentane yellow crystals of **m-3b** (0.036 g, 47%). Anal. Calcd for $C_{21}H_{34}IrP$: C, 49.49; H, 6.72. Found: C, 49.37; H, 6.69.

Cp*Ir(PMe₃)(Me)(*o*-C₆H₄Me) (o-3b**).** According to the above procedure, Cp*Ir(PMe₃)(Me)(Cl) (0.061 g, 0.13 mmol) was reacted with (*o*-C₆H₄Me)MgBr (0.5 mL of a 2 M solution in diethyl ether, 1 mmol) to give yellow crystals of **o-3b** (0.027 g, 39%). Anal. Calcd for $C_{21}H_{34}IrP$: C, 49.49; H, 6.72. Found: C, 49.44; H, 6.74.

Thermolysis of 1a in Benzene. **1a** (0.02 g) and benzene (1 mL), or benzene-*d*₆ when the reaction was monitored by ¹H NMR spectroscopy, were loaded into an NMR tube, and the tube was sealed off under argon. It was then immersed in a thermostated oil bath. The progress of the reaction was evaluated by monitoring the signal of CH₃D [δ 0.13 (t, *J*(HD) 2 Hz)] and the integrated intensities of the Cp* resonances for **1a** (δ 1.40), **2a** (δ 1.34), and **10** (δ 1.32). After 2 weeks at temperatures below 70 °C, no reaction was found to occur. After **1a** was heated in benzene for 12 days at 110 ± 0.5 °C, the tube was cracked open, the solvent was removed, and benzene-*d*₆ was added. The ¹H NMR spectrum revealed a mixture of **1a** (10%), **2a** (24%), and **10** (66%).

Under the same conditions, **1a** was reacted with toluene or toluene-*d*₈ to give the *m*- and *p*-tolyl derivatives **3a** (2/1, 95%) and with trifluorotoluene to give the diaryl derivatives.

Reaction of Cp*Ir(PPh₃)Me₂ (1a**) with Cp₂Fe⁺PF₆[−] in Dichloromethane-*d*₂: Formation of Cp*Ir(C₆H₄PPh₂)Me (**12**).** **1a** (0.038 g, 0.062 mmol) in dichloromethane-*d*₂ (2 mL) was treated in an NMR tube with Cp₂Fe⁺PF₆[−] (6 × 10^{−3} mmol). After a few seconds, a gas was evolved from the surface of the solid oxidant, which was shown to be CH₄ by GLC and ¹H NMR (δ 0.2), while signals due to **1a** decreased to give a new product. The reaction was complete in 30 min. The solution was filtered and dried under vacuum. Crystallization from pentane at −30 °C gave yellow crystals of **12** (0.028 g, 75%).

Reaction of Cp*Ir(PPh₃)Me₂ (1a**) with Cp₂Fe⁺PF₆[−] in Benzene: Formation of Cp*Ir(C₆H₄PPh₂)Me (**12**) and Cp*Ir(PPh₃)(Me)(Ph) (**2a**).** **1a** (0.02 g, 0.032 mmol) and Cp₂Fe⁺PF₆[−] (1.1 mg, 0.0032 mmol) were reacted similarly in

benzene or, when the reaction was monitored by ¹H NMR spectroscopy, in benzene-*d*₆ using hexamethylbenzene as internal standard. CH₄ (δ 0.14) was evolved, and **1a** was converted with 92% yield after 2 h to a mixture of the orthometalated compound **12** (15%) and the methyl phenyl derivative Cp*Ir(PPh₃)(Me)(Ph) (**2a**) (85%), both identified by comparison of the ¹H NMR spectral data with those of an authentic sample prepared as described above. The same equilibrium composition was obtained by reacting pure **12** or **2a** with Cp₂Fe⁺PF₆[−] or AgBF₄ in benzene.

Reaction of Cp*Ir(PMe₃)Me₂ (1b**) with Cp₂Fe⁺PF₆[−] in Benzene: Formation of Cp*Ir(PMe₃)(Me)(Ph) (**2b**).** The reaction was carried out as described for **1a**, except that the conversion of **1b** (0.042 g, 0.097 mmol) was complete in 1 h. The solution was separated from the oxidant by filtration and pumped to dryness. Crystallization from pentane at −30 °C gave yellow crystals of **2b** (0.041 g, 85%).

The isotope effect ($k_H/k_D = 2.2$) was evaluated by carrying out the reaction in benzene/benzene-*d*₆ mixtures of different compositions (1/1, 2.5/1, and 4/1) and comparing the ¹H NMR signals' integrated areas of the phosphine and pentamethylcyclopentadienyl ligand of **3b** and **3b-d₅ to those of the phenyl group.**

ESR Spectral Studies of the Chemical Oxidation of 1a, 1b, 13, and 14. The reaction mixtures were prepared by placing a weighed amount of metal complex (typically, 5 mg) and AgBF₄ (1 mg) into a quartz tube (o.d. 3 mm; i.d. 2 mm) fitted with a quartz–Pyrex joint and a Corning Rotaflo Teflon tap (DISA, Milan). The tube was then attached to a vacuum line and degassed by standard vacuum/argon techniques; afterward, it was immersed in a dry ice-cooled acetone bath and then charged with dichloromethane under pure argon atmosphere. The hyperfine coupling constants and line widths were obtained by computer simulation of the ESR spectra.

Acknowledgment. We thank the CNR (Rome) for financial support.

OM950070S